Pore-scale experimental study of carbonated water injection in an oil-wet carbonate: an improved insight into wettability alteration and displacement mechanisms

Ziqiang Qin[1,*], *Maziar* Arshadi[1], and *Mohammad* Piri[1]

[1]Department of Petroleum Engineering, University of Wyoming, Laramie, Wyoming 82071, United States

Abstract. Carbonated water injection (CWI) has been proposed to mitigate the poor sweep efficiency of conventional CO_2 flooding. Furthermore, CWI requires much less CO_2 that makes it more attractive for EOR projects that have access to limited quantities of CO_2. Even though previous experimental studies have presented data supporting the effectiveness of CWI for enhanced oil recovery, the direct evidences obtained from naturally-occurring rock samples on pore-scale displacement mechanisms responsible for the observed recovery enhancements are scarce. In the past decade, X-ray microtomography (micro-CT) technology has become more readily available and this has created numerous opportunities for pore-level investigations of complex multi-phase flow processes in natural porous media. In this study, we probed the displacement mechanisms taking place during CWI and subsequent depressurization processes through miniature core-flooding experiments at elevated pressure and temperature conditions (1400 psi and 50 °C), using a HPHT core-flooding system integrated with a high-resolution micro-CT scanner. The miniature core sample was dynamically aged with crude oil at initial water saturation and subsequently subjected to waterflooding, CWI, and a depressurization step. The sample was repeatedly imaged using the micro-CT scanner in the course of the experiments. The images were then processed to generate three-dimensional fluid occupancy maps from which the fluid saturations, in-situ contact angles, and local displacement patterns were determined. The results showed a significant incremental oil recovery due to CWI and subsequent depressurization steps compared to the unadulterated waterflooding. In-situ contact angle measurements yielded direct evidences of wettability alteration from oil-wet to neutral-wet conditions during CWI. Our observations indicated that the wettability alteration was a gradual process, which facilitates oil displacement from the medium. The swelling of oil during CWI and the displacements taking place during the subsequent depressurization process also contributed to oil production.

1 Introduction

CO_2 injection is a well-established enhanced oil recovery (EOR) scheme in oil reservoirs. However, a viscous fingering effect has always been a technical challenge for continuous CO_2 injection, which is amplified in carbonate reservoirs. This is mainly due to the complex pore network structure and heterogeneity of carbonate rocks [1,2]. Furthermore, most of the carbonate reservoirs were found to be in mix-wet or even oil-wet conditions [3]. Carbonated water injection (CWI) has been proposed to mitigate the poor sweep efficiency of continuous CO_2 flooding. In addition, CWI is an economically-efficient EOR strategy as only a small amount of CO_2 is consumed in this method.

Kechut et al. [4] provided experimental results showing that CWI could lead to higher oil recovery compared to unadulterated waterflooding in both secondary and tertiary modes. Also, 45%-51% of the injected CO_2 was stored in the porous medium at the end of the experiments, which indicates that the CWI EOR strategy could also serve for a CO_2 storage purpose. Sohrabi et al. [5] showed a recovery enhancement due to CWI through a series of core-flooding experiments. They reported that secondary CWI led to higher and faster oil recovery compared to that of tertiary CWI. It was also concluded that the CO_2 was moving ahead of the carbonated water (CW) front, which indicates successful delivery of CO_2 by the CW. Seyyedi et al. [6] investigated the potential of CW for enhancing the water imbibition rate and oil recovery utilizing high-pressure imbibition experiments. They reported that CW could increase the oil recovery of spontaneous imbibition in both sandstone and carbonate rocks. The oil recovery factor was a function of the initial wettability state of the rocks.

In the later period of oil production processes, CWI schemes could also result in an additional oil recovery during reservoir pressure decline stages. Riazi et al. [7] performed experiments using high-pressure micromodels and showed that a pressure blow-down period subsequent to CWI could lead to further oil production. They claimed that CO_2 exsolution during the depressurization caused

* Corresponding author: zqin@uwyo.edu

local flow diversions and the coalescence of isolated oil clusters, which resulted in additional oil recovery. Zuo and Benson [8] also studied the effect of depressurization after CWI on oil recovery in micromodels. They reported that a 10% additional oil recovery was achieved after reducing the pore pressure 2 MPa below the CO_2 liberation pressure. The main mechanisms governing the additional oil recovery were that exsolved CO_2 blocked the water flow channels and diverted the flow of water into the oil-filled pores. Alizadeh et al. [9] reported that CO_2 exsolution after CWI, as a result of depletion, led to remarkable oil recovery. A 34.6% additional recovery of the original oil in place was achieved in their experiments.

Even though previous experimental studies have presented data supporting the effectiveness of CWI for EOR and have proposed possible underlying mechanisms, the direct evidence obtained from oil-wet carbonate rocks on pore-scale displacement mechanisms responsible for the observed recovery enhancements are scarce. In the past decade, X-ray microtomography (micro-CT) technology has become more readily available, and this has created numerous opportunities for pore-level investigations of complex multi-phase flow processes in natural porous media [10]. High-resolution X-ray images have been used for capillary pressure measurements [11], in-situ contact angle measurements [12, 13, 14], relative permeability determination [15], and quantitative characterization of pore space [16]. In this study, we investigated the wettability alteration and displacement mechanisms taking place during CWI and subsequent depressurization processes through miniature core-flooding experiments at elevated pressure and temperature conditions (1400 psi and 50 °C), using a HPHT core-flooding system integrated with a high-resolution micro-CT scanner. The potential wettability alteration was probed by in-situ contact angle measurement methods. Pore-fluid occupancy maps were utilized to analyse the pore-scale displacement mechanisms.

2 Experiments

2.1 Rock and fluid properties

The rock sample used in this study was a type of carbonate outcrops named Fond du Lac. A miniature sample, 8.9 mm in diameter and 44.5 mm in length, was drilled from a rock block. The sample was dried at 110 °C for 24 hours in an oven and subsequently cooled down to the room temperature in a desiccator before use. The sample was scanned by a micro-CT scanner, and a porosity of 10.05% was calculated based on the histogram-thresholding method. An absolute brine permeability of 45 mD was measured following Darcy's law.

Brine solution was prepared using distilled water, 0.5 wt% $CaCl_2$, and 19 wt% NaI. To avoid dissolution of the carbonate matrix during flow tests, a sacrificial core plug was immersed in the brine solution for 24 hours. The connate brine and brine used for unadulterated waterflooding shared the same composition. Brine was degassed for one hour before use. Carbonated water was prepared by mixing pure CO_2 (with a purity higher than 99.9%) with the degassed brine in a high-pressure cell at the reservoir conditions (50 °C and 1400 psi). CW was circulated in the cell for one day and then rested for three days to make sure that CO_2 was fully dissolved into the brine. Crude oil was collected from an oil reservoir located in the Permian basin, Taxes, USA. The oil was filtered through a 0.5 μm filter to remove possible residue and debris [17]. Next, the oil was tagged with 12 vol% 1-iodooctane to ensure sufficient X-ray attenuation contrast between fluids in the micro-CT images (Figure 1). Table 1 provides the fluid properties.

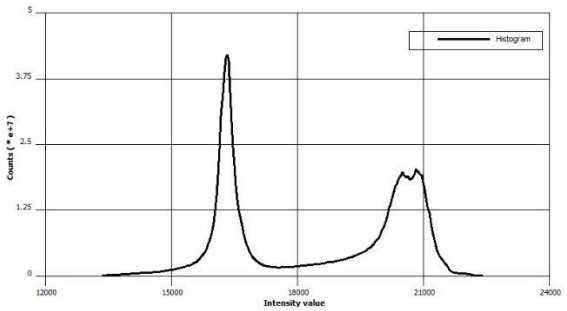

Fig. 1. Grey level histogram of the fluid occupancy maps at the end of the unadulterated waterflooding.

Table 1. Brine and crude oil properties.

Fluids	Viscosity* (cP)	Density* (g/ml)	Salinity (ppm)	Asphaltene content (%)
Brine	1.15	1.17	242236	-
Crude oil	6.5	0.85	-	0.9

* Viscosity and density properties were measured at ambient conditions.

2.2 Experimental apparatus

Flow experiments were performed using a reservoir-condition three-phase core-flooding apparatus integrated with a high-resolution X-ray micro-CT scanner. The equilibrium cell was used to prepare CW at the reservoir conditions. The core-holder was made out of carbon fibre to minimize X-ray attenuation. During the experiments, the core-holder was mounted vertically inside the CT chamber.

The X-ray imaging system was a Thermo Fisher heliscan Micro-CT scanner. Scanning was performed by collecting X-ray projections at different angles while the sample was rotating. The scanning parameters were appropriately selected to optimize image quality (Table 2). Figure 2 shows a schematic diagram of the experimental apparatus used in this study and the details of the system were explained elsewhere [18].

Table 2. X-ray microtomography parameters used in this study

X-ray current (uA)	X-ray voltage (kV)	Number of projections	Exposure time (s)	Voxel size (micron)	Scanning time (hours)
53.3	100	2880	1	3.23	8.3

2.3 Experimental procedure

The core sample was placed inside the core-holder with a confining pressure of 200 psi. Gaseous CO_2 was injected into the sample for 30 minutes to remove the bulk air from the porous medium. Then, the system was vacuumed for 24 hours. In the meantime, the sample was scanned by the micro-CT scanner to collect a set of dry reference images. Subsequently, the core was fully saturated with brine by injecting 50 pore volumes of the fluid. Afterward, the pore pressure and the confining pressure were simultaneously increased to 1400 psi and 1600 psi, respectively. The system temperature was also raised to 50 °C at this stage by adjusting the thermo-controller of the heating tape surrounding the core holder. Accordingly, brine was injected into the sample at different flow rates of 0.01 cc/min, 0.02 cc/min, 0.03 cc/min, and 0.04 cc/min to measure the absolute brine permeability. The flow rate was changed when the differential pressure across the core became stable. Next, the system was rested for five days to achieve an ironic equilibrium between the rock surface and the brine. Afterward, primary drainage was performed by injecting crude oil into the core at a constant flow rate of 0.03 cc/min. After the pressure drop across the core stabilized, the core was scanned and the initial brine saturation was determined based on image analysis. The sample was then dynamic aged with crude oil at the initial water saturation by injecting oil at a low flow rate of 0.0006 cc/min. The core was scanned frequently during aging to monitor the evolution of oil-brine contact angles. The aging process was considered complete once the in-situ oil-brine contact angles did not change further.

Subsequently, an unadulterated waterflooding was conducted with a brine injection rate of 0.005 cc/min. The experiment was further continued with a CWI step at the same flow rate as that of the unadulterated waterflooding. The core was repeatedly scanned during these processes and both flooding steps were terminated when the pore-fluid occupancy maps remained constant (a total of 15PV of CW were injected). Afterward, the injection side of the core-holder was closed. The back pressure (initially at 1400 psi) was reduced in steps to allow CO_2 exsolution, which represented the reservoir pressure decline during

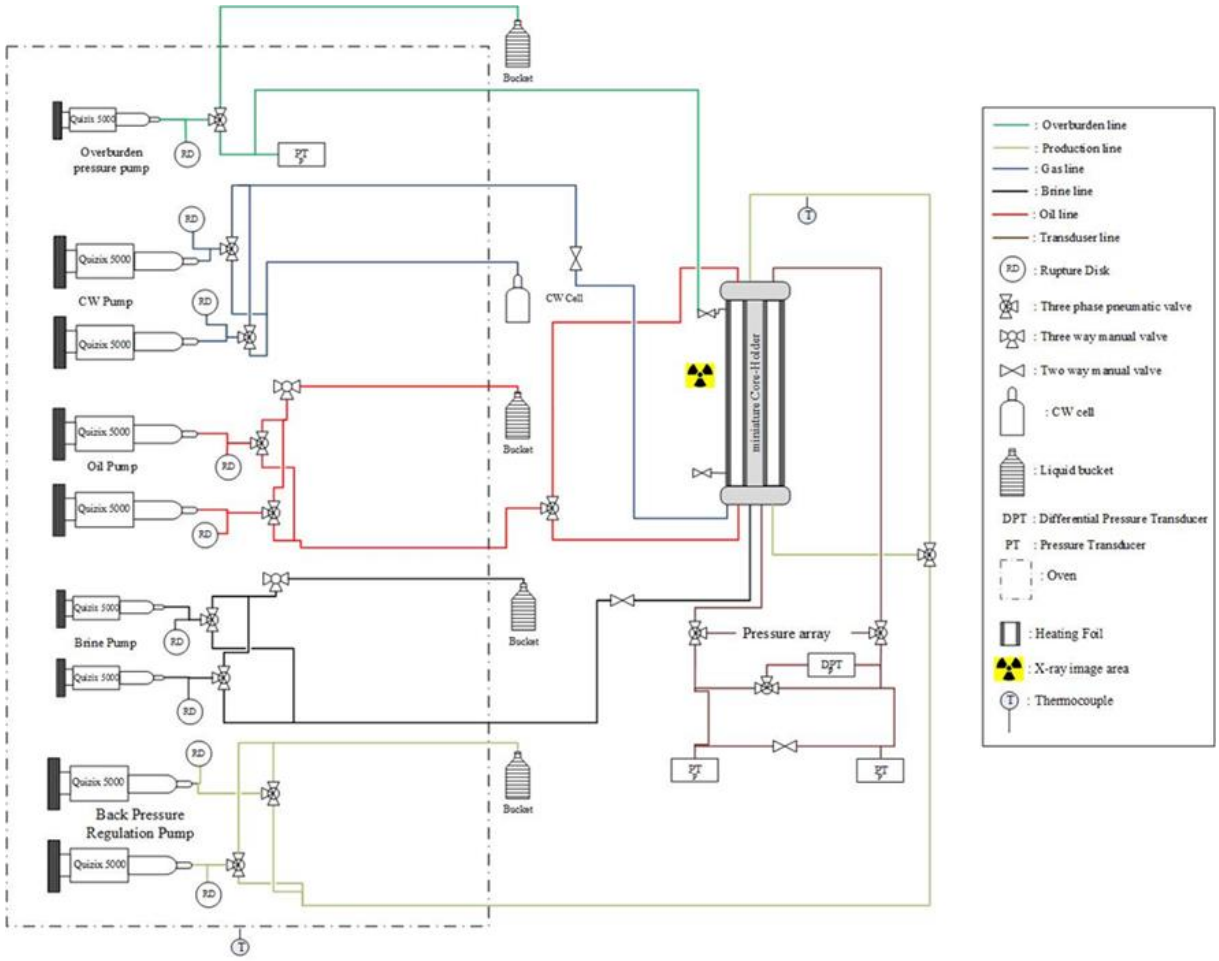

Fig. 2. A schematic diagram of the experimental apparatus.

depletion periods. The confining pressure was decreased at the same time to maintain the net confining pressure at 200 psi. This was done to avoid any possible pore structure deformation, as the primary focus of this study was to investigate the potential wettability alteration and displacement mechanisms of CWI and subsequent depressurization processes. The core sample was scanned at various pressure intervals during the depressurization stage. The middle part of the sample was scanned during the experiments to avoid possible end effects in the field of view (9.3mm*9.3mm*6.59mm). The projections collected during scanning were reconstructed to generate three-dimensional internal structures of the rock and residing fluids. Avizo 9.4.0 and PerGeos 1.7.0 software platforms were utilized to visualize and further process the raw images. The details of image processing workflow were explained elsewhere [13]. Figure 3 illustrates various steps of this workflow.

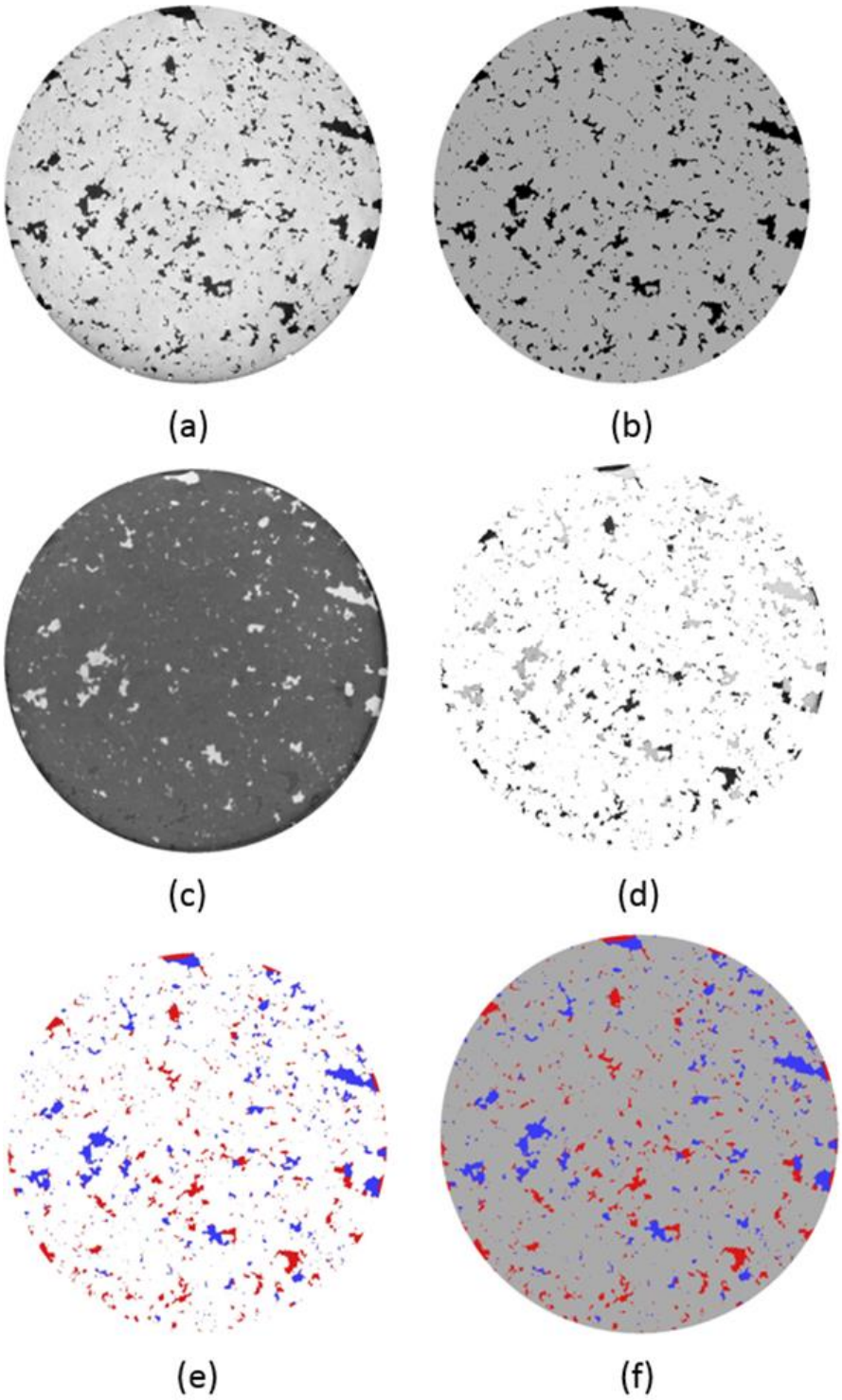

Fig. 3. The workflow of image processing methods: (a) filtered reference image, (b) pore map obtained from the reference image, (c) filtered flooded image, (d) multiplied image, (e) segmented pore-fluid occupancy map, (f) segmented rock-fluid system (brine: blue, oil: red, and grain: grey).

* Corresponding author: zqin@uwyo.edu

3 Results and Discussion

3.1 In-situ saturations

To quantify the effectiveness of CWI and subsequent depressurization processes for EOR, we calculated the fluid saturations from the segmented pore-fluid occupancy maps of various flooding stages. The initial brine saturation was 0.173 at the end of the aging process. After fifteen pore volumes of unadulterated waterflooding, the remaining oil saturation reached to 0.483, which translates to an oil recovery of 41.6%. After fifteen pore volumes of CWI, the in-situ oil saturation was reduced to 0.397 and did not change further. This is equivalent to an oil recovery of 52%. Therefore, CWI resulted in 10.4% additional recovery of original-oil-in-place compared to that at the end of the unadulterated waterflooding. Subsequently, the back pressure was reduced in steps to mimic the reservoir depletion process in later stages of production. The exsolution of CO_2 led to a reduction in remaining oil saturation to 0.334 as the back pressure was reduced to 130 psi. The residual oil saturation ultimately reached to 0.21 as the back pressure was further reduced to 40 psi, which corresponds to an ultimate oil recovery of 74.6%. In other words, an additional oil recovery of 22.6% was achieved as a result of the pressure blow-down process. Therefore, one can conclude that the depressurization after CWI also significantly contributed to EOR. Figure 4 demonstrates the variations of remaining oil saturation and oil recovery with respect to different flooding stages.

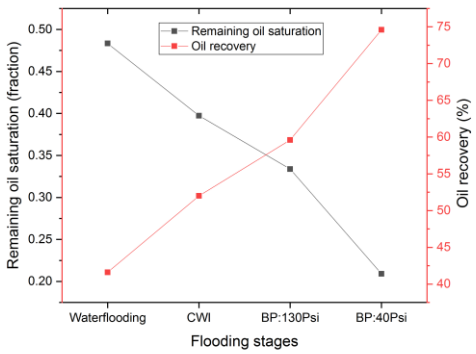

Fig. 4. Variations of remaining oil saturation and oil recovery with respect to different flooding stages.

3.2 In-situ characterization of wettability

To probe the potential wettability alteration caused by CWI, the in-situ oil-brine contact angles were measured on segmented pore-fluid occupancy maps during aging, unadulterated waterflooding, CWI, and subsequent depressurization processes. In each dataset, 30 contact angles were measured at randomly-selected locations to characterize the local wettability heterogeneity and reduce the human error. In-situ contact angle measurements might have an absolute error value of two degrees as a result of uncertainties with identifying fluid-fluid and rock-fluid interfaces and the details of this highly-accurate in-situ contact angle measurement technique were explained elsewhere [13]. The average oil-brine contact angle at the end of the unadulterated waterflood was 118.76°, which is similar to the average value of 118.15° after aging. This similarity indicates that no wettability alteration occurred during the unadulterated waterflooding process. In contrast, the average oil-brine contact angle had been reduced to 111.09° after one pore volume of CWI. The average value had reached to 107.02° after fifteen pore volumes of CWI, which reveals that the wettability alteration towards increasing water-wetness had occurred due to the CWI. The oil-brine contact angle values further decreased as the experiment was continued. At 1100 psi pore pressure during depressurization, the average oil-brine contact angle was 104.82°. This value was ultimately reduced to 95.89° by the end of the depressurization stage (i.e., 40 psi pore pressure). Our observations indicate the CW-induced wettability alteration is a gradual process that could, at least partially, impact the pore-scale mechanisms of oil recovery during CWI.

3.3 Pore-scale displacement mechanisms of CWI and subsequent depressurization process

Characterization of fluid occupancy maps revealed that the wettability alteration facilitated the oil displacement during CWI as a result of the increase in threshold capillary pressures (negative values in an oil-wet system). Figure 5 demonstrates the evolution of pore-fluid occupancy maps at the end of the unadulterated waterflooding (with an average oil-brine contact angle of 118.76°) and CWI (with an average oil-brine contact angle of 107.02°).

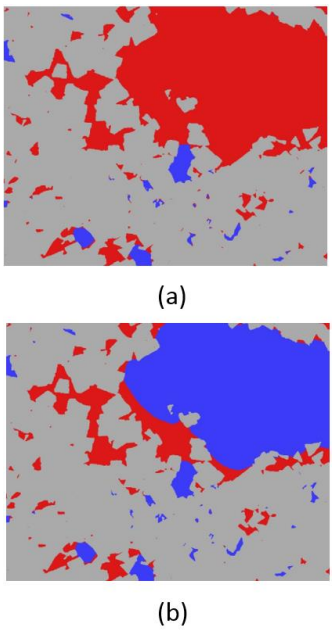

Fig. 5. Exemplary two-dimensional maps of fluid occupancy at the end of the (a) unadulterated waterflooding and (b) CWI (brine: blue, oil: red, and grain: grey).

Furthermore, based on in-situ fluid occupancy investigation, we found that the swelling of oil ganglia (possibly due to the diffusion of CO_2 from the injected CW to the oil phase) also contributed to oil production. Moreover, during the subsequent depressurization process, the displacements taking placed significantly changed the fluid occupancies and resulted in additional oil recovery. Further image analysis is being carried out at this moment to provide more insight into the pore-scale displacement mechanisms governing the observed recovery enhancements (Figure 6).

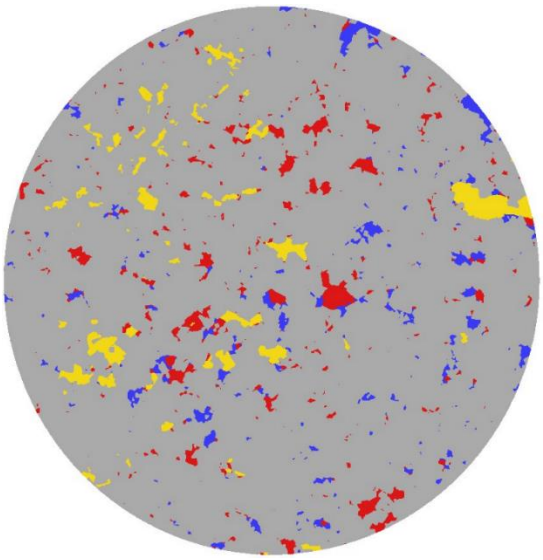

Fig. 6. Exemplary two-dimensional maps of fluid occupancy at the end of the depressurization process (gas: yellow, brine: blue, oil: red, and grain: grey).

4 Summary and conclusion

In this study, we probed the wettability alteration and displacement mechanisms taking place during CWI and subsequent depressurization processes through miniature core-flooding experiments at elevated pressure and temperature conditions, using a HPHT core-flooding system integrated with a high-resolution micro-CT scanner. The potential wettability alteration was characterized through an in-situ contact angle measurement method. Pore-fluid occupancy maps were utilized to investigate the pore-scale displacement mechanisms of CWI. Here, we summarize the main findings:

1) A significant amount of additional oil recovery was achieved during the CWI and subsequent depressurization processes compared to the unadulterated waterflooding.
2) Wettability alteration towards increasing water-wetness occurred as a result of CWI. The wettability alteration was a gradual process, which facilitates oil displacement from the medium.

The authors gratefully acknowledge the financial support of Thermo Fisher Scientific Company, Hess corporation, and the School of Energy Resources at the University of Wyoming.

References

1. J. Lai, et al. "Prediction of reservoir quality in carbonates via porosity spectrum from image logs." Journal of Petroleum Science and Engineering **173** (2019): 197-208.
2. J. Lai, et al. "Pore structure and fractal characteristics of Ordovician Majiagou carbonate reservoirs in Ordos Basin, China." AAPG Bulletin 20,190,412 (2019).
3. P. Zhang, and T. Austad. "Wettability and oil recovery from carbonates: Effects of temperature and potential determining ions." Colloids and Surfaces A: Physicochemical and Engineering Aspects **279**.1-3 (2006): 179-187.
4. NI Kechut, M. Sohrabi, and M. Jamiolahmady. "Experimental and numerical evaluation of carbonated water injection (CWI) for improved oil recovery and CO2 storage." *SPE EUROPEC/EAGE Annual Conference and Exhibition*. Society of Petroleum Engineers, 2011.
5. M. Sohrabi et al. "Coreflooding studies to investigate the potential of carbonated water injection as an injection strategy for improved oil recovery and CO 2 storage." Transport in porous media **91**.1 (2012): 101-121.
6. M. Seyyedi and M. Sohrabi. "Enhancing water imbibition rate and oil recovery by carbonated water in carbonate and sandstone rocks." Energy & Fuels **30**.1 (2015): 285-293.
7. M. Riazi, M. Sohrabi, and M. Jamiolahmady. "Experimental study of pore-scale mechanisms of carbonated water injection." Transport in porous media **86**.1 (2011): 73-86.
8. L. Zuo, and S. M. Benson. "Exsolution enhanced oil recovery with concurrent CO2 sequestration." Energy Procedia **37** (2013): 6957-6963.
9. A. H. Alizadeh. et al. "Multi-scale experimental study of carbonated water injection: an effective process for mobilization and recovery of trapped oil." Fuel **132** (2014): 219-235.
10. J. Lai et al. "Three-dimensional quantitative fracture analysis of tight gas sandstones using industrial computed tomography." Scientific reports **7**.1 (2017): 1825.
11. R.T. Armstrong, M.L. Porter, and D. Wildenschild. "Linking pore-scale interfacial curvature to column-scale capillary pressure." Advances in Water Resources **46** (2012): 55-62.
12. M. Andrew, B. Bijeljic, and M.J. Blunt. "Pore-scale contact angle measurements at reservoir conditions using X-ray microtomography." Advances in Water Resources **68** (2014): 24-31.

13. Z. Qin, M. Arshadi, and M. Piri, “Micro-scale experimental investigations of multiphase flow in oil-wet carbonates. I. In-situ wettability and low-salinity waterflooding.” Fuel (to be published)
14. Z. Qin, M. Arshadi, and M. Piri, “Micro-scale experimental investigations of multiphase flow in oil-wet carbonates. II. Tertiary gas injection and WAG.” Fuel (to be published)
15. J. M. Schembre, and A. R. Kovscek. "A technique for measuring two-phase relative permeability in porous media via X-ray CT measurements." Journal of Petroleum Science and Engineering **39**.1-2 (2003): 159-174.
16. S. Youssef, et al. "Quantitative 3D characterisation of the pore space of real rocks: improved μ-CT resolution and pore extraction methodology." *Int. Sym. of the Society of Core Analysts* (2007).
17. W. Kuang, S. Saraji, and M. Piri. "A systematic experimental investigation on the synergistic effects of aqueous nanofluids on interfacial properties and their implications for enhanced oil recovery." Fuel **220** (2018): 849-870.
18. Z. Qin, M. Arshadi, and M. Piri, "Pore-scale experimental investigation of in-situ wettability and displacement mechanisms governing WAG in oil-wet carbonates." *Int. Sym. of the Society of Core Analysts* (2019).